Sensors and Materials, Vol. 35, No. 8 (2023) 2871–2880
MYU Tokyo

S & M 3361

Optical and Electrical Properties of ITO:Ga/Ag Double-layer Thin Films for Photosensor Applications

Yen-Chen Chang,[1] Tao-Hsing Chen,[2*] Tsai-Dan Chang,[2]
Sheng-Lung Tu,[1] and Yun-Hwei Shen[1]

[1]Department of Resources Engineering, National Cheng Kung University, Tainan City 701, Taiwan
[2]Department of Mechanical Engineering, National Kaohsiung University of Science and Technology, No. 415, Jiangong Rd., Sanmin Dist., Kaohsiung City 807618, Taiwan

(Received February 14, 2023; accepted April 11, 2023; online published April 25, 2023)

Keywords: sputtering, ITO:Ga, annealing, optical and electrical properties, multilayer

In this study, double-layer transparent conductive thin films are formed by depositing silver (Ag) of 99.99% purity on a glass substrate by direct-current (DC) magnetron sputtering, then forming an oxide layer on the Ag layer by depositing gallium-doped indium tin oxide (ITO:Ga) with an ITO:Ga ratio of 97:3 by radio-frequency magnetron sputtering. The films are annealed in vacuum at different temperatures to rearrange the crystals in the films and thereby reduce the defect density. The thicknesses, electrical properties, optical properties, surface structures, and figures of merit (FOMs) of the ITO:Ga/Ag double-layer thin films before and after annealing are analyzed. It is found that the resistivity of the double-layer thin films decreases with increasing annealing temperature and that the lowest resistivity is 5.03×10^{-5} Ω-cm and the highest average transmittance is 73.33% for the specimen annealed at 450 °C, which also has the highest FOM of 5.31×10^{3} Ω^{-1}. The ITO:Ga/Ag double-layer thin films have excellent optical and electrical properties for photosensor applications.

1. Introduction

Transparent conductive oxide (TCO) films exhibit high electrical conductivity and transmittance, are highly reflective in the IR spectral region, and have high current carrier concentration (typically about 10^{20} cm^{-3}). These outstanding properties allow TCO films to be widely used in a variety of photoelectric devices such as solar cells, thin-film transistors, organic light-emitting devices, and flat-panel displays.[1–3] Currently, the major TCO film materials are zinc oxide (ZnO), indium (III) oxide (In_2O_3), titanium dioxide (TiO_2), tin (IV) oxide (SnO_2), and cadmium oxide (CdO). To increase the conductivity of TCO films, it is common practice to dope the film materials with either a group-III element, such as Al, Ga, or In, or a group-IV element, such as Si, Sn, Ti, or Zr.[4–11] Doping with a certain amount of a metal element increases the current carrier concentration and causes an increase and a subsequent decrease in Hall mobility. Once a critical amount of dopant is reached, however, the resistivity will increase. In addition to

*Corresponding author: e-mail: thchen@nkust.edu.tw
https://doi.org/10.18494/SAM4354

ISSN 0914-4935
https://myukk.org/

doping with a metal element, reasonably high conductivity can be achieved by forming a multilayer (e.g., TCO:metal/metal) film and annealing the film.[12,13] Generally, a metal element is opaque to visible light, but if the thickness of a metal film is controlled at 100 Å or less, the metal film will be permeable to visible light and highly reflective in the IR spectral region.[14] In the pursuit of higher optical transmittance and electrical performance, many recent studies have proposed the formation of a metal/oxide double-layer film structure comprising an oxide film and a metal film.[15–18] Such double-layer films are configured to suppress the reflection of visible light by the metal layer and therefore have relatively high transmittance.[19] It has also been shown that a metal film of less than 15 nm thickness tends to form an island film, that a multilayer film formed with such a metal film and an oxide film can be annealed to inhibit the formation of the island structure by the metal film, and that the thermal diffusion during annealing enables strong bonding between the oxide film and the metal film, which contributes to increased conductivity and optical transmittance.

A film can be prepared by a physical or chemical method. Physical film formation methods include vacuum evaporation, sputtering, and ion-assisted deposition, whereas chemical film formation methods include the sol-gel method and chemical vapor deposition.[20–24] In this study, we used magnetron sputtering to deposit the constituent layers of gallium-doped indium tin oxide/silver (ITO:Ga/Ag) double-layer thin films because this method allows not only the manufacturing process to be highly controllable but also uniform films to be easily obtained. Then, the electrical and optical properties of the ITO:Ga/Ag double-layer thin films before and after annealing were analyzed to identify the most suitable processing parameters. All the results in this study can be employed in photosensor applications.

2. Experimental Procedure

The experiment involved changing parameters and conditions such as the sputtering power and annealing temperature to form a number of ITO:Ga/Ag multilayer thin films on Corning glass. The target materials used in the experiment were an ITO:Ga alloy with an ITO:Ga ratio of 97:3 and Ag of 99.99% purity. The processing parameters selected for the ITO:Ga layer were a power of 80 W, a constant pressure of 6 mTorr, a gas flow rate of 15 sccm Ar, and a sputtering time of 30 min. The sputtering parameters for the Ag layer were a power of 20 W, a sputtering time of 1 min, and a constant pressure of 6 mTorr. An α-step profilometer (KLA-Tencor) was used to measure the film thickness. The annealing temperature was set at 200–450 °C. To analyze the multilayer films, the structural phase was identified with an X-ray diffractometer (XRD, Siemens D-500), the conductivity and optical transmittance were measured with a Hall effect measuring instrument (AHM-800B) and a UV-VIS spectrophotometer (Hitachi 2900), respectively, and the surface topography was observed by scanning electron microscopy (SEM, JSM-7000F).

3. Results and Discussion

3.1 Film thicknesses

The thicknesses of a double-layer film sample and its ITO:Ga and Ag layers are shown in Table 1. The annealing process did not change the thicknesses significantly; changes were only about ±2 nm, which had little effect on film properties. Moreover, the error of the profilometer was about 10–20 nm, which is much larger than the change in thickness caused by annealing; therefore, the change in film thickness after annealing will not be discussed further.

3.2 XRD spectra of thin-film crystal structure

Figure 1 shows the properties of the ITO:Ga/Ag double-layer thin films under test. The unannealed double-layer thin film and the film annealed at 200 °C were in an amorphous state (i.e., no crystalline phase was found in the film). No significant In_2O_3 peak was observed for these two films, which may be attributed to the even distribution of Ag ions in the In_2O_3 lattices. It is known from Ref. 25 that an amorphous ITO only exhibits a minor peak at $2\theta \approx 30.5°$; thus, it can be inferred that the peak around 38° in this study corresponds to the (111) face of Ag. Moreover, according to Ref. 26, ITO crystallizes at about 150–200 °C. In this study, the crystallization was relatively slow and incomplete when the annealing temperature was 200 °C. When the annealing temperature was increased, the main diffraction peak of (222) at the film surface became increasingly prominent. When the annealing temperature was increased to 300 and 400 °C, the multilayer films became fully polycrystalline. The completely annealed ITO layer only showed a preferential (222) orientation.

The crystalline phase began to appear in the ITO:Ga/Ag double-layer thin films when the annealing temperature was 300 °C. The (222), (400), (411), (431), (440), and (622) peaks were

Table 1
Thicknesses of a double-layer film.

Oxide layer	ITO:Ga (61.71 nm)
Metal layer	Ag (14.7 nm)
Total thickness	76.41 nm

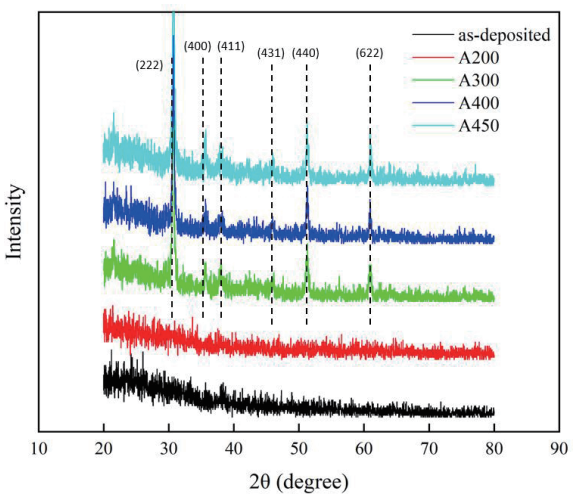

Fig. 1. (Color online) XRD spectra of ITO:Ga/Ag annealed at different temperatures.

found at 30.05, 35.4, 37.6, 45.5, 50.9, and 62.1°, respectively, but all the peaks correspond to In_2O_3, meaning that Ag ions might have been substituted and thereby incorporated into the In_2O_3 lattices, with (222) being the major growth direction. Peaks with the highest intensity appeared when the annealing temperature was 400 °C.

3.3 Electrical properties of films annealed at different temperatures

The electrical performance of the ITO:Ga/Ag double-layer thin films under test is shown in Table 2. It was found that the resistivity of the thin films decreased with increasing annealing temperature. The lowest resistivity, i.e., 5.03×10^{-5} Ω-cm, was obtained at the annealing temperature of 450 °C. During annealing, Ag diffused and was substituted into the oxide layer. It is speculated that a higher annealing temperature promoted the diffusion of Ag into the ITO thin film because the heat energy assisted electrons to pass the conduction bond barrier.

It can be seen from the XRD spectra in Fig. 1 that the unannealed ITO:Ga/Ag double-layer thin film and the film annealed at 200 °C were amorphous, from which it can be inferred that the crystal grains in these two films were still in the growth stage. When the annealing temperature was 300 °C, the In_2O_3 peak appeared and the resistivity decreased to 6.38×10^{-5} Ω-cm, the main cause being the change the carrier concentration. When the annealing temperature was 450 °C, the resistivity decreased to 5.03×10^{-5} Ω-cm. It is speculated that Ag was doped into the In_2O_3 lattices at this temperature. Only the In_2O_3 peak appeared in the XRD spectra.

3.4 Optical properties of films annealed at different temperatures

As can be seen in Figs. 2 and 3, which respectively show the changes in the optical transmittance and energy gap of the double-layer thin films after annealing, the double-layer thin films with a Ag layer had an average transmittance of about 68–73% and the transmittance increased slightly with the annealing temperature.

The energy gap was calculated using the following optical band gap equation:[27]

$$(\alpha h\upsilon)^2 = A(h\upsilon - Eg), \tag{1}$$

Table 2
Electrical performance of ITO:Ga/Ag double-layer thin films annealed at different temperatures.

ITO:Ga/Ag: ITO:Ga 80 W 30 min/Ag 20 W 1 min			
Annealing temperature (°C)	Resistivity (Ω-cm)	Mobility (cm^2/Vs)	Carrier concentration (cm^{-3})
As-deposited	6.58×10^{-5}	5.46	2.12×10^{21}
200	6.49×10^{-5}	6.29	2.21×10^{21}
300	6.38×10^{-5}	11.7	3.01×10^{21}
400	6.09×10^{-5}	19	4.10×10^{21}
450	5.03×10^{-5}	245	5.07×10^{21}

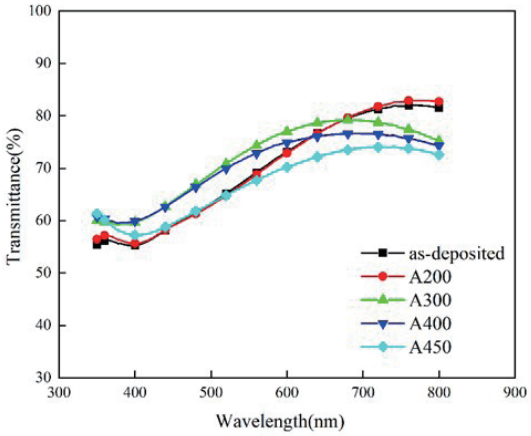

Fig. 2. (Color online) Transmittances of ITO:Ga/Ag annealed at different temperatures.

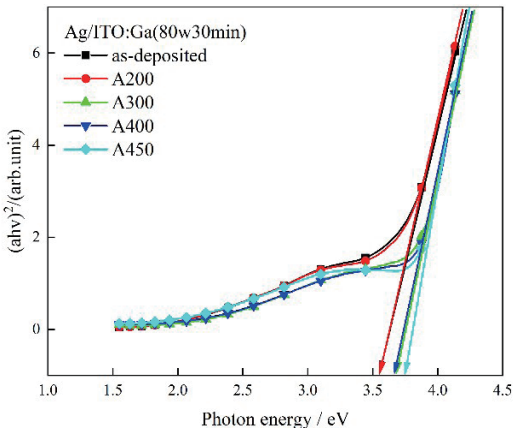

Fig. 3. (Color online) Energy gaps of ITO:Ga/Ag annealed at different temperatures.

where A is a constant and α and $h\upsilon$ are the absorption coefficient of the film and the energy of the incident radiation, respectively. The energy gap of the unannealed double-layer film was 3.64 eV. When the annealing temperature was 450 °C, the energy gap reached its maximum value of 3.79 eV.

The average transmittance of the ITO:Ga/Ag films increased with the annealing temperature, and the highest transmittance of 73.33% occurred when the annealing temperature was 450 °C. The main cause of this phenomenon was that, as the annealing temperature increased, the metal atoms in the metal layer were able to be doped into and substitute for the oxide atoms in the oxide layer after receiving sufficient energy. As a result, the reflection of visible light by the metal layer was reduced. It was found that the energy gap gradually increased with the annealing temperature. The ITO:Ga/Ag film annealed at 450 °C had the largest energy gap of 3.79 eV. At the largest energy gap, an electron can have more energy and increase the conduction band level. The resistivity also decreases owing to the high carrier concentration.

3.5 Surface topography of films annealed at different temperatures

The surface topography of the ITO:Ga/Ag double-layer thin films annealed at different temperatures was analyzed by SEM. Figure 4 presents the surface topography of the double-layer thin films. After annealing, the film surface had a denser texture and, as can be seen in the surface topography images, was free of surface defects such as holes and cracks. As can also be seen, the films had a flatter surface and a denser texture when the annealing temperature was increased. Relatively large crystal grains were formed on the surface of the ITO:Ga/Ag double-layer thin films, which was mainly because of the dopant metal (i.e., Ag) layer. However, all the films had a flat surface and a dense texture regardless of the annealing temperature.

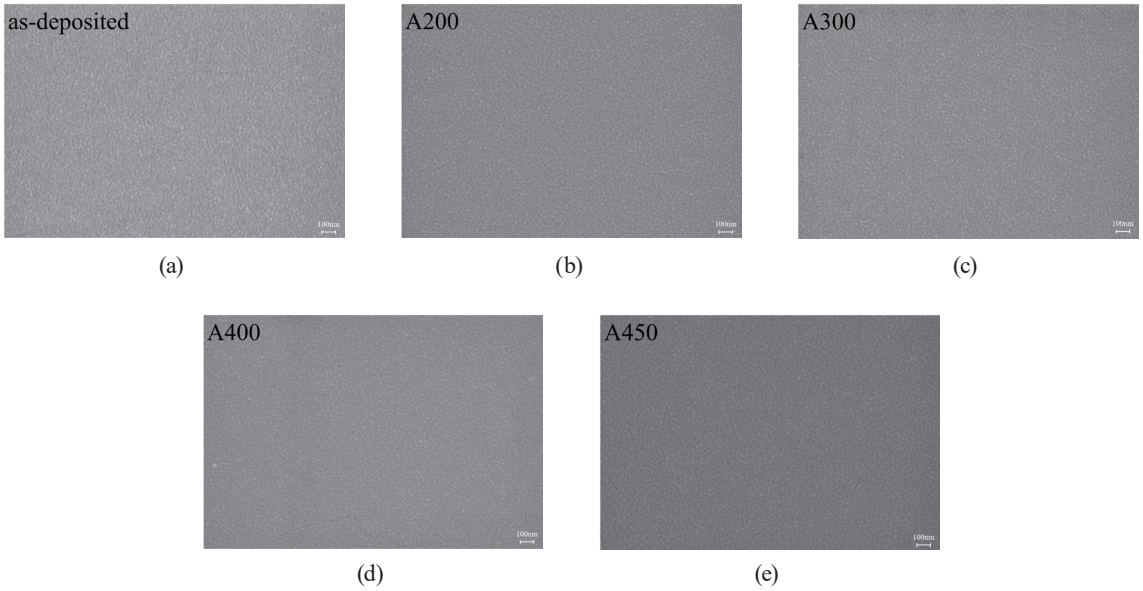

Fig. 4. Surface features of ITO:Ga/Ag double-layer thin films annealed at different temperatures: as-deposited (a) and annealed at (b) 200, (c) 300, (d) 400, and (e) 450 °C.

3.6 Figures of merit of films before and after annealing

The quality of transparent conductive films can be expressed by the figure of merit (FOM) to facilitate comparison, where the FOM is calculated from the resistivity and transmittance. Table 3 presents the FOMs of the double-layer thin films annealed at different temperatures. As can be seen from Eq. (2), the FOM is directly proportional to the transmittance to the power of 10. Therefore, transmittance is a critical factor determining the FOM of such films. A high FOM requires relatively low resistivity and high transmittance.[28]

$$\Phi_{TC} = \frac{T_{av}^{10}}{R_{sh}} \tag{2}$$

From Table 3, it can be observed that the FOM increased with the annealing temperature. The highest FOM, i.e., $5.31 \times 10^3\ \Omega^{-1}$, was observed for the annealing temperature of 450 °C. When the annealing temperature increased, the transmittance also increased, which resulted in an increased FOM.

3.7 Crystal grain sizes of films after annealing

The crystal grain size was calculated by substituting the peak value in the XRD spectra into Scherrer's formula to obtain the full width at half maximum (FWHM). Scherrer's formula is[29]

Table 3
FOMs of double-layer thin films annealed at different temperatures.

FOM Φ_{TC} (Ω^{-1})	
Annealing temperature (°C)	ITO:Ga/Ag
As-deposited	4.15×10^3
200	4.28×10^3
300	4.42×10^3
400	4.62×10^3
450	5.31×10^3

Table 4
Crystal grain sizes and FWHM values of double-layer thin films annealed at different temperatures.

ITO:Ga/Ag		
Annealing temperature (°C)	FWHM	Grain size (nm)
300	0.285	26.90
400	0.271	30.43
450	0.225	36.65

$$D = \frac{0.9\lambda}{\beta \cos\theta}, \tag{3}$$

where D is the grain size, λ is the wavelength of the incident X-ray, i.e., 0.15418 nm, θ is the angle of the incident light, and β is the FWHM. As λ and θ are fixed, D and β are reciprocals of each other; the smaller the FWHM, the larger the grain size.[30] Table 4 presents the crystal grain sizes and FWHM values of the ITO:Ga/Ag double-layer thin films annealed at different temperatures. No grain size or FWHM value is shown for the unannealed double-layer thin film or for the film annealed at 200 °C because no crystals were found in those films. Crystallization began when the annealing temperature was 300 °C, and the FWHM decreased with increasing annealing temperature. As a result, the crystal grain size gradually increased from 26.90 to 36.65 nm as the annealing temperature increased from 300 to 450 °C.

4. Conclusion

In this study, the ITO:Ga/Ag double-layer thin films were deposited by the RF sputter magnetron sputtering technology and annealed at temperatures of 200, 300, 400 and 450 °C. According to our experimental results, the overall thickness of the ITO:Ga/Ag double-layer thin films barely changed with the annealing temperature. From the XRD spectra, we found that the ITO:Ga/Ag double-layer thin films were amorphous before and after annealing at 200 °C. A crystalline phase formed when the annealing temperature was 300 °C, but all the peaks corresponded to In_2O_3, meaning that Ag ions might have been substituted and thereby incorporated into the In_2O_3 lattices, with (222) being the major growth direction. The largest peak value appeared when the annealing temperature was 450 °C. The ITO:Ga/Ag double-layer thin films exhibited improved optical and electrical properties with increasing annealing temperature. The lowest resistivity of the thin films of 5.03×10^{-5} Ω-cm and the highest transmittance of 73.33% were observed at the annealing temperature of 450 °C. Furthermore, the largest energy gap of 3.79 eV appeared when the annealing temperature was 450 °C. The highest FOM of the ITO:Ga/Ag double-layer thin films of 5.31×10^3 Ω^{-1} was also observed at the annealing temperature of 450 °C because the annealed thin film had the lowest resistivity and high transmittance. Moreover, the crystalline ITO:Ga/Ag double-layer thin films grew at a sufficiently high annealing temperature. It can be seen that the annealing temperature is an important factor for improving the optical and electrical properties of the thin films.

Acknowledgments

This paper was finished through Research Project MOST111-2628-E-992-001-MY2, which is supported by the National Science and Technology Council of Taiwan. The authors would like to express their gratitude to the National Science and Technology Council for its support, which enabled the smooth completion of this research. The authors also gratefully acknowledge the use of EM000700 of MOST 110-2731-M-006-001, which belongs to the Core Facility Center of National Cheng Kung University.

References

1 C.-F. Liu, T.-H. Chen, and J.-T. Huang: Sens. Mater. **32** (2020) 3727. https://doi.org/10.18494/SAM.2020.3138
2 T. Wang, H.-P. Ma, J.-G. Yang, J.-T. Zhu, H. Zhang, J. Feng, S.-J. Ding, H-L. Lu, and D. W. Zhang: J. Alloy Compd. **744** (2018) 381. https://doi.org/10.1016/j.jallcom.2018.02.115
3 C. Cao, A. Zhou, S. Mu, G. Zhang, X. Song, and Z. Sun: Mater. Sci. Eng. B **176** (2011) 1430. https://doi.org/10.1016/j.mseb.2011.07.027
4 T.-H. Chen, T.-C. Cheng, and Z.-R. Hu: Microsyst. Technol. **19** (2013) 1787. https://doi.org/10.1007/s00542-013-1837-5
5 M.-Y. Yen, T.-H. Chen, P.-H. Lai, S.-L. Tu, and Y.-H. Shen: Sens. Mater. **33** (2021) 3941. https://doi.org/10.18494/SAM.2021.3706
6 B. Zhang, X. P. Dong, X. F. Xu, X. J. Wang, and J. S. Wu: Mater. Sci. Semicond. Process **10** (2007) 264 https://doi.org/10.1016/j.mssp.2008.03.003
7 T.-H. Chen and C.-L. Yang: Opt. Quantum Electron. **48** (2016) 533. https://doi.org/10.1007/s11082-016-0808-3
8 T.-H. Chen and T.-Y. Chen: Nanomater. **5** (2015) 1831. https://doi.org/10.3390/nano5041831
9 V. Sharma, R. Vyas, P. Bazylewski, G. S. Chang, K. Asokan, and K. Sachdev: RSC Adv. **6** (2016) 29135. https://doi.org/10.1039/c5ra24422f
10 A. V. Moholkar, S. M. Pawar, K. Y. Rajpure, C. H. Bhosale, and J. H. Kim: Appl. Surf. Sci. **255** (2009) 9358. https://doi.org/10.1016/j.apsusc.2009.07.035
11 S. Singh, V. Sharma, and K. Sachdev: J. Mater. Sci. **52** (2017) 11580. https://doi.org/10.1007/s10853-017-1328-7
12 K. P. Sibin, G. Srinivas, H. D. Shashikala, A. Dey, N. Sridhara, A. K. Sharma, and H. C. Barshilia: Sol. Energy Mater. Sol. Cells **172** (2017) 277. https://doi.org/10.1016/j.solmat.2017.08.001
13 Y.-S. Park, K.-H. Choi, and H.-K. Kim: J. Phys. D. Appl. Phys. **42** (2009) 1. https://doi.org/10.1088/0022-3727/42/23/235109
14 B. Parida, Y. Gil, and H. Kim: J Nanosci. Nanotechnol. **19** (2019) 1455 https://doi.org/10.1166/jnn.2019.16242
15 M. Acosta, J. Mendez-Gamboa, I. Riech, C. Acosta, and M. Zambrano: Superlattice. Microst. **127** (2019) 49. https://doi.org/10.1016/j.spmi.2018.03.018
16 H.-W. Wu and C.-H. Chu: Mater. Lett. **105** (2013) 65. https://doi.org/10.1016/j.matlet.2013.04.017
17 M. Y. Yen, T. H. Chen, P. H. Lai, S. L. Tu, Y. H. Shen, and C.-C. Huang: Sens. Mater. **34** (2022) 175. https://doi.org/10.18494/SAM3555
18 D. Miao, S. Jiang, S. Shang, and Z. Chen: Ceram. Int. **40** (2014) 12847. https://doi.org/10.1016/j.ceramint.2014.04.139
19 E. Bertran, C. Corbella, M. Vives, A. Pinyol, C. Person, and I. Porqueras: Ceram Intl **165** (2003) 139. https://doi.org/10.1016/j.ssi.2003.08.055.
20 D. R. Sahu, S.-Y. Lin, and J.-L. Huang: Appl. Surf. Sci. **252** (2006) 7509. https://doi.org/10.1016/j.apsusc.2005.09.021.
21 P. Thilakan, S. Kalainathan, J. Kumar, and P. Ramasamy: J. Electron. Mater. **24** (1995) 719. https://doi.org/10.1007/BF02659730
22 M. J. Alam and D. C. Cameron: J. Vac. Sci. Technol. A **19** (2001) 1642. https://doi.org/10.1116/1.1340659
23 M. Purica, E. Budianu, E. Rusu, M. Danila, and R. Gavrila: Thin Solid Films **403**–**404** (2002) 485. https://doi.org/10.1016/S0040-6090(01)01544-9
24 A. J. C. Fiddes, K. Durose, A. W. Brinkman, J. Woods, P. D. Coates, and A. J. Banister: J. Cryst. Growth, **159** (1996) 210. https://doi.org/10.1016/0022-0248(95)00707-5
25 J. A. Jeong and H. K. Kim: Sol. Energy Mater. Sol. Cells **93** (2009) 1891. https://doi.org/10.1016/j.solmat.2009.06.014.

26 S. Y. Lee, E. S. Cho, and S. J. Kwon: Appl. Surf. Sci. **487** (2019) 990. https://doi.org/10.1016/j.apsusc.2019.05.106
27 T. Minami, H. Nanto, and S. Takata: J. Appl. Phys. **24** (1985) L605. https://doi.org/10.1143/JJAP.24.L605
28 G. Haacke: J Appl Phys, **47** (1976) 4086. https://doi.org/10.1063/1.323240
29 M. Caglar, S. Ilican, and Y Caglar: Thin Solid Films **517** (2009) 5023. https://doi.org/10.1016/j.tsf.2009.03.037
30 E. Muchuweni, T. S. Sathiaraj, and H. Nyakotyo: Ceram Int **42** (2016) 10066. https://doi.org/10.1016/j.ceramint.2016.03.110

About the Authors

Yen-Chen Chang received an executive master of business administration (EMBA) degree from National Sun Yat-Sen University in 2013. She has been a Ph.D. student under the resources engineering program of National Chen Kung University since 2017. She is also a general manager of an environment cleaning company.

Tao-Hsing Chen received his B.S. degree from National Cheng Kung University, Taiwan, in 1999 and his M.S. and Ph.D. degrees from the Department of Mechanical Engineering, National Cheng Kung University, in 2001 and 2008, respectively. From August 2008 to July 2010, he was a postdoctoral researcher at the Center for Micro/Nano Science and Technology, National Cheng Kung University. In August 2010, he became an assistant professor at National Kaohsiung University of Applied Sciences (renamed National Kaohsiung University of Science and Technology), Taiwan. Since 2016, he has been a professor at National Kaohsiung University of Science and Technology. His research interests are in metal materials, TCO thin films, thermal sensors, and photosensors. (thchen@nkust.edu.tw)

Tsai-Dan Chang received her B.S. degree from National Kaohsiung University of Science and Technology, Taiwan, where she is currently studying for her M.S. degree. Her research interests are in TCO thin film, materials engineering, and sensors.

Sheng-Lung Tu received his M.S. degree from the Department of Mechanical Engineering, National Cheng Kung University, in 2010 and his Ph.D. degree from the Department of Resources Engineering, National Cheng Kung University, in 2014. Since 2014, he has worked as a general affairs officer at National Cheng Kung University. His research interests are in PVD technology, thin film technology, and sensors.

Yun-Hwei Shen received his B.S. degree from the Department of Mineral and Petroleum Engineering, National Cheng Kung University, in 1982, his M.S. degree in mineral preparation engineering from the University of Alaska Fairbanks, USA, in 1987, and his Ph.D. degree from the Department of Environmental Engineering, Penn. State University, USA, in 1992. Since 1999, he has been a professor at the Department of Resources Engineering, National Cheng Kung University. His research interests are in catalysis technology, hydrometallurgical processing of resource materials, sensors, and hydrometallurgical processes.